REPORT DOCUMENTATION PAGE

Form Approved
OMB No. 0704-0188

1. REPORT DATE *(DD-MM-YYYY)*
31-01-2005

REPRINT

4. TITLE AND SUBTITLE
Survey of DSCS-III B-7 Differential Surface Charging

5a. CONTRACT NUMBER

5b. GRANT NUMBER

5c. PROGRAM ELEMENT NUMBER

6. AUTHOR(S)
L.H. Krause*, D.L. Cooke, C.L. Enloe*, G.I. Font*,
M.G. McHarg*, V. Putz*, K.P. Ray, and M.J. Toth, Jr.*

5d. PROJECT NUMBER
5021

5e. TASK NUMBER
RS

5f. WORK UNIT NUMBER
A1

7. PERFORMING ORGANIZATION NAME(S) AND ADDRESS(ES)
Air Force Research Laboratory/VSBXR
29 Randolph Road
Hanscom AFB MA 01731-3010

8. PERFORMING ORGANIZATION REPORT NUMBER
AFRL-VS-HA-TR-2005-1011

9. SPONSORING / MONITORING AGENCY NAME(S) AND ADDRESS(ES)

10. SPONSOR/MONITOR'S ACRONYM(S)
AFRL/VSBXR

11. SPONSOR/MONITOR'S REPORT NUMBER(S)

12. DISTRIBUTION / AVAILABILITY STATEMENT
Approved for Public Release; Distribution Unlimited.

*Dept Physics, US Air Force Academy, CO

13. SUPPLEMENTARY NOTES
REPRINTED FROM: IEEE TRANSACTIONS ON NUCLEAR SCIENCES, Vol 51, No. 6, pp 3399-3407, Dec 2004.

14. ABSTRACT
An analysis of differential charging between dielectric surface materials and the frame of a DSCS-III geosynchronous spacecraft is presented. Charging levels measured by surface potential monitors (SPMs) covered with samples of Kapton and Astroquartz have been recorded for one half of a solar cycle. Both seasonal and solar cycle effects are seen in the daily peak levels of the SPM voltages, with local maxima occurring near the equinoxes and a general trend increasing as solar max is approached. Charge neutralization by an onboard Xe plasma contractor was demonstrated to be effective throughout the mission, with a mean voltage reduction of 86% for Astroquartz and 74% for Kapton. Though a statistical analysis shows a general correlation between the fluence of charging electrons with SPM voltages, the event-specific correlation contains enough variance to cast doubt on the usefulness of an electron sensor as a differential charging alarm. We have found that a Kapton-covered SPM may be better suited than an electron sensor as a differential charging alarm.

15. SUBJECT TERMS
Geosynchronous orbit Satellite charging Space environmental effects
Space weather

16. SECURITY CLASSIFICATION OF:			**17. LIMITATION OF ABSTRACT**	**18. NUMBER OF PAGES**	**19a. NAME OF RESPONSIBLE PERSON**
a. REPORT UNCLAS	UNCLAS	**c. THIS PAGE** UNCLAS	SAR	9	Kevin P. Ray
					19b. TELEPHONE NUMBER *(include area code)* 781-377-3828

Survey of DSCS-III B-7 Differential Surface Charging

Linda Habash Krause, David L. Cooke, C. Lon Enloe, Gabriel I. Font, M. Geoff McHarg, Victor Putz, Kevin P. Ray, and Michael J. Toth, Jr.

Abstract—**An analysis of differential charging between dielectric surface materials and the frame of a DSCS-III geosynchronous spacecraft is presented. Charging levels measured by surface potential monitors (SPMs) covered with samples of Kapton and Astroquartz have been recorded for one half of a solar cycle. Both seasonal and solar cycle effects are seen in the daily peak levels of the SPM voltages, with local maxima occurring near the equinoxes and a general trend increasing as solar max is approached. Charge neutralization by an onboard Xe plasma contactor was demonstrated to be effective throughout the mission, with a mean voltage reduction of 86% for Astroquartz and 74% for Kapton. Though a statistical analysis shows a general correlation between the fluence of charging electrons with SPM voltages, the event-specific correlation contains enough variance to cast doubt on the usefulness of an electron sensor as a differential charging alarm. We have found that a Kapton-covered SPM may be better suited than an electron sensor as a differential charging alarm.**

Index Terms—**Geosynchronous orbit, satellite charging, space environmental effects, space weather.**

I. Introduction

DURING the last few decades, several laboratory and on-orbit experiments have made progress in the investigation of space vehicle properties and environmental conditions that instigate spacecraft charging and the subsequent anomalous behavior of the vehicle's systems resulting from such charging. Spacecraft charging can appear in many forms, including frame charging, which characterizes the frame-to-plasma potential difference, and differential charging, which characterizes frame-to-surface or intersurface potential differences. Static charge regularly accumulates on dielectric surfaces in a low-density plasma, such as that of geosynchronous earth orbit (GEO), resulting in frequent differential charging events of GEO spacecraft that commonly use dielectric materials as protective coverings (e.g., for thermal control). The effects of differential charging can be particularly problematic to space vehicle electrical systems; a significant potential difference between two materials in close proximity to each other may generate an electric field that exceeds the material-dependent breakdown voltage, leading to arc discharging [1]. These discharges have resulted in noise pulses that propagate through the vehicle's electrical systems, causing malfunctions and system interruptions [2].

It is necessary to develop a suitable understanding of the processes associated with charging and discharging of dielectric materials in the space environment in order to devise and employ mitigation techniques to prevent or ameliorate the effects of differential charging. It is well known that the probability of a spacecraft experiencing either frame or differential charging depends on the spacecraft design, its exposure to sunlight (both immediate and long-term), and the local neutral and plasma environment surrounding the spacecraft. Since geomagnetic activity leads to modification of the geosynchronous plasma environment, several previous studies have focused on linking magnetic storm and magnetospheric substorm activity directly with the frame charging of the geosynchronous Defense Satellite and Communication System (DSCS) III [3]–[5]. Whereas it has been found that a statistical approach can suggest a significant charging probability given minimum levels of activity, as represented with the disturbance storm time index (Dst), the planetary index ap, and the polar cap index (PCI), there was no combination of threshold values of these parameters that would provide an accurate frame charging warning system [4].

Investigation of the problem of differential surface charging requires consideration of the engineering design of the spacecraft, materials degradation from exposure to sunlight and space radiation, and the physics and chemistry of the plasma interacting with the spacecraft surface. Several missions have flown with the intent of investigating such interactions; interestingly, at least one of the experiments aboard such spacecraft failed due to an electrostatic discharge event [6]. In 1995, the U.S. Air Force launched the geosynchronous DSCS-III B-7, which carried a surface charging diagnostic and mitigation experiment called the Charge Control System (CCS) [7]. Differential charging data were accumulated for two dielectric materials common to spacecraft: Astroquartz fabric and Kapton film. Each of these materials was placed over a surface potential monitor (SPM), which recorded the voltage between the material and the spacecraft frame. The CCS was designed to determine levels of differential charging and use those levels as a trigger to activate a Xe plasma source to quench the charging events. The autonomous operation of this system was demonstrated successfully for almost six years of operation on orbit. In a preliminary survey of differential charging events, [8] showed that over a three-yearperiod, maximum differential charging voltages of the Astroquartz sample peaked at 3500 V in the absence of the plasma source, yet the sample only

Manuscript received July 19, 2004. This work was supported by the Air Force Office of Scientific Research.

L. Habash Krause, C. L. Enloe, G. I. Font, M. G. McHarg, V. Putz, and M. J. Toth are with the Department of Physics, U.S. Air Force Academy, CO 80840 USA (e-mail: Linda.Krause@usafa.af.mil).

D. L. Cooke and K. P. Ray are with the Space Vehicles Directorate, Air Force Research Laboratory, Hanscom AFB, MA 07131.

Digital Object Identifier 10.1109/TNS.2004.840838

reached 1200 V when the source was activated. In the present investigation, the authors conduct a rigorous survey of the differential charging events over the six years (1995–2001) of data collected by the DSCS-III B-7 CCS experiment. In particular, we investigate the efficacy of charge neutralization for each material and how this efficacy evolves with time due to changes in the material properties and/or the plasma source characteristics. Additionally, we seek a significant correlation (if any) between incident electron fluxes and the charging of the dielectrics in the hopes of determining whether or not an electron sensor may be used as a charging alarm.

The paper is organized as follows. Section II presents a background on differential charging, along with a review of previous experiments. The DSCS-III B-7 satellite and the instrumentation employed in the CCS experiment are described in Section III. Observations of spacecraft differential charging as seen through SPM voltages are presented in Section IV. Section V contains the statistical data and analysis of the differential charging events and the efficacy of neutralization by the plasma contactor. The paper concludes with a brief summary of findings in Section VI.

II. Background: Differential Charging

Differential surface charging, defined here as the development of a potential difference between a dielectric surface and the conductive frame of the spacecraft, occurs when the surface is irradiated with electrons that have energies of $\sim$ 10 keV. In this case, the electrons penetrate to depths where secondaries are generated deep enough in the material and which are too low in energy to be ejected from the material, resulting in a net negative charge deposition and a consequential negative static charge buildup. Specifically, previous studies have shown that electrons primarily within the energy range from 20–50 keV are responsible for significant differential surface charging [9]. Incident electrons with energies less than this range would generate secondaries that are able to escape the material, contributing to the so-called "self-balancing" of electron fluxes that was observed on Spacecraft Charging at High Altitudes (SCATHA); those with energies greater than this range would penetrate through the material without completely being stopped within, thus avoiding contribution to the net charge deposition in the material.

The dielectric materials under consideration typically have a small conductivity that allows for conduction current to flow. However, the incident electron flux is properly treated as a pure scattering problem, independent of conductivity. Even though electric fields are generated by the presence of static charge build up within the material, the collisional stopping power in these materials is always greater than the breakdown electric field within the material. Thus, even if there was enough static charge built up to generate electric fields capable of appreciable deceleration of incoming electrons, the material could not support the electric fields against electrostatic discharge (ESD); these ESDs would occur long before the electric fields had any effect on the incoming electrons.

Material conductivity is important, however: the electrostatic fields drive a conduction current via the charge carriers within the material that serves to cancel (at least partially) the incoming electron flux. The conduction current is dominated by the dark current, and as long as the material thickness is greater than the penetration depth of the incident electrons, the balance of these two currents in steady state allows for the computation of the electric potential of the surface, in accordance with the following equation [10]:

$$J_{\text{incident}} + J_{\text{emitted}} - \sigma \frac{V_s - V_g}{d} = 0$$

where J_{incident} is the incident electron current density (A/cm^2), and J_{emitted} is the electron current density ejected from the surface due to electron impact ionization or photoionization if the material is exposed to sunlight. The third term is the conduction current, where σ is the dark conductivity, V_s is the potential of the charged surface, V_g is the spacecraft frame potential, and d is the thickness of the dielectric material. Here, $V_s - V_g$ is the voltage that quantifies differential charging of a material.

Because the material's dark conductivity plays a critical role in the establishment of a steady-state surface potential, specification of this material parameter is crucial in the prediction of surface charging of various surfaces. The situation is complicated by the fact that some materials have properties that are altered by exposure to the space environment. In particular, the dark conductivity of Kapton, a polymide film used extensively on spacecraft in GEO, increases upon exposure to sunlight and particle radiation in space [11]. When irradiated by these sources, polymetric bonds can be broken and subsequent chemical reactions can increase surface conductivity. The enhanced conductivity can persist in the absence of atomic oxygen (e.g., characteristic of the GEO environment). Specifically, the increase of Kapton's dark conductivity has been observed both on-orbit with SCATHA measurements, as inferred from a reduction in differential charging during the latter part of the mission, and in the laboratory. [12] reported that the differential charging voltage of the Kapton-covered SPM aboard SCATHA decreased by "orders of magnitude" after its first year on orbit. In the laboratory, Leung and Kan [13] found that current-voltage (I-V) curves for unexposed Kapton exhibited dark currents that were three orders of magnitude smaller than those for photo-exposed Kapton. It should be noted that there will be no appreciable change in the surface potential of a dielectric with time of exposure to space radiation if the bulk material current is small compared to the incident charging current. Here, the surface potential is dominated by the secondary electron emission from the surface and not the dark current. This is not the result that was observed on SCATHA—clearly, the bulk current must have been large (or comparable to) the incident charging current.

Astroquartz also exhibits usual behavior under certain environmental conditions. It was observed during the SCATHA mission that the quartz fabric charged up to significantly higher surface potentials than those observed in preflight laboratory tests. Generally, when a "well-behaved" insulator is irradiated with a constant and uniform electron source, the material will charge up exponentially with time, then remain at a constant potential, indicating that the conduction current has increased sufficiently to balance the incident electron flux. With postflight

laboratory tests, it was found that quartz did follow this pattern for low-density beams (0.08 nA/cm^2). However, the preflight tests were conducted with higher density beams (0.5–1.5 nA/cm^2). With these higher beam densities, the voltage instead increased rapidly until a peak was reached, and then it decayed exponentially over time. The exponential voltage decay is due to electrostatic discharges. When the incoming current is greater than the conduction current, electric fields are generated in the material, which are great enough to cause breakdown. Furthermore, higher beam voltages and lower densities result in a more rapid decay, indicating that the discharge mechanism is due to secondary electron emission from SiO_2 surface. It is understood that quartz has this unique characteristic because it is quite porous and has a large surface area to volume ratio. This allows secondaries created deep in the surface to diffuse out of the material while the less mobile holes are fixed in place. Indeed, lower voltages were observed during preflight laboratory tests than those on orbit; smaller preflight ground-based charging results were initially obtained because currents during the initial tests were higher than those on orbit. The large on-orbit voltage observed during a particularly severe storm was the result of having a small enough incident current to allow the voltage to exponentially reach a constant value while being large enough to impart a significant amount of static charge—thus resulting in a large charging level.

III. DSCS-III B-7 Mission Description

DSCS-III is comprised of ten satellites located in geosynchronous orbit (i.e., with an orbital radius of 6.6 earth radii). DSCS-III B-7 is an operational, three-axis stabilized satellite located at 52.5° west longitude [3], resulting in a midnight Mission Local Time (MLT) corresponding to 03:30 Universal Time (UT). The DSCS Charge Control System experiment resides on the satellite, and its only active component, a Xe plasma contactor, is allowed to operate for up to 1 h each day. The passive components are allowed to operate at all MLTs, allowing continuous coverage of particle observations and discrete surface potentials and therefore spacecraft frame and differential charging.

A. DSCS CCS Instrumentation

The CCS is based in part upon the Flight Model Discharge System (FMDS) developed by Hughes Research Laboratories, Malibu, CA [14]. The FMDS is a standalone system that monitors spacecraft potential and autonomously activates a plasma contactor for neutralization of electrically charged surfaces. The components of the FMDS that comprise the DSCS CCS include 1) SPMs, designed to determine differential charging of a dielectric material relative to the spacecraft frame potential; 2) an active Xe plasma contactor; and 3) power electronics required to operate and control the plasma contactor. Additionally, electrostatic analyzers (ESAs) are used to measure electron and ion populations in the vicinity of the spacecraft. The instrumentation is described in detail below.

B. Surface Potential Monitors

The DSCS CCS incorporates two SPMs, one covered with General Electric Astroquartz fiberglass fabric type 171A4676TY8, and the other covered with General Electric polymide film coated with Indium-Tin-Oxide (ITO) (i.e., Dupont Kapton H) and aluminized on the back surface. These dielectric materials were selected based on their frequency of use as thermal control surfaces on geosynchronous spacecraft. The Astroquartz fabric is approximately 0.3 mm (12 mil) thick, whereas the Kapton film is approximately 0.05 mm (2 mil) thick. The stopping powers for 20–50-keV electrons in Astroquartz and Kapton are found using the Bethe–Block formalism (e.g., [15]), with extremes that range from 15 MeV · cm^2/g for the 20-keV electrons in Kapton to 5 MeV · cm^2/g for the 50-keV electrons in Astroquartz. With mass densities of 1.4 g/cm^3 for Kapton and 2.2 g/cm^3 for Astroquartz, the electron penetration depths under consideration vary from 4.9–24 μm in Astroquartz and 6.7–34 μm in Kapton. Thus, the materials have thicknesses greater than the penetration range of the electrons with energies under consideration with this experiment, resulting in the necessity of the conduction (i.e., dark) current to contribute significantly to balancing the charging current from electron irradiation.

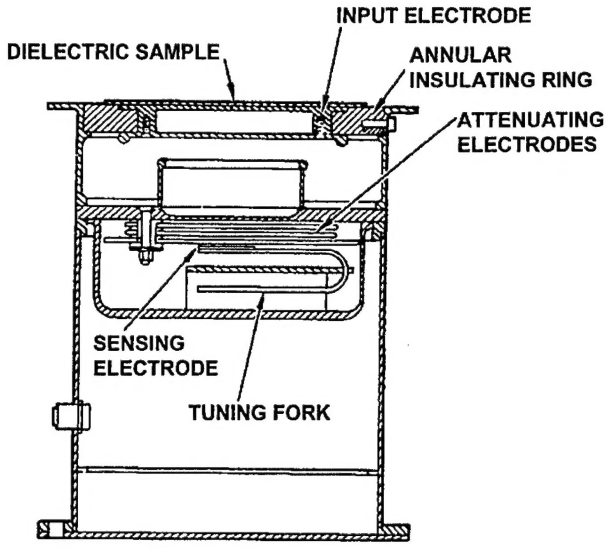

Fig. 1. Schematic of SPM [14].

With the exception of the material coverings, the two DSCS SPMs are designed identically. In the design of the SPM, care was taken to avoid alteration of the charged dielectric by the operation of the instrument, thus requiring an electric field transducer with a functionally infinite input impedance. The design was based on the National Aeronautics and Space Administration's surface voltage sensor [16] that incorporates a closed-loop feedback sensing system that detects a null in the field-sensing probe when it is at the same potential as the charged surface. A combination of electrodes attenuated the field resulting from the charged dielectric surface, allowing the null to be achieved with a low-voltage (±10-V) feedback signal. The SPM design is shown in Fig. 1. The dielectric covering is bonded to the input electrode and annular insulating ring, precluding direct exposure of the electrode to the space plasma environment. The annular ring electrically isolates the dielectric covered electrode from the rest of the instrument. The potential measurement of the dielectric surface is made indirectly by the input electrode

which is capacitively coupled to the front surface of the dielectric covering. A negative charge buildup on the attenuating electrodes results in a positive charge buildup on the sensing electrode attached to a tuning fork. The tuning fork is forced to oscillate during the sensor measurement, producing a sinusoidal increase and decrease of the induced charge on the sensing electrode. The mechanical oscillation of the tuning fork results in a changing capacitance, producing an alternating current signal which, when integrated and amplified, is fed back to the system as a standard potential that matches the measured potential. In this manner, a null-difference between reference and measured potentials is achieved.

C. Xe Plasma Contactor

The CCS plasma contactor is a low-energy (< 40-eV) Xe plasma source that incorporates a hollow cathode design. Electrons are thermionically boiled off of the interior surface of the hollow cathode, made from a low-work-function material, and subsequently impact-ionize Xe gas that flows through the cathode tube. The ionized inert gas then flows out of the plasma contactor with axial energy low enough that allows the charged particles to be attracted to charged surfaces of the spacecraft, thus neutralizing (at least in part) differential charge build up between isolated dielectric surfaces or between individual dielectric surfaces and the spacecraft frame. Additionally, because the spacecraft is essentially capacitively coupled to the ambient space plasma, the plasma contactor has the effect of improving the direct current (dc) connection to the plasma environment by creating an electrically conducting conduit between the two. This effects neutralization of a frame-charged spacecraft since the increased dc conductivity allows charge to flow more freely from the ambient plasma to a spacecraft, thus bringing the spacecraft's floating potential down toward the ambient plasma potential. Though the plasma contactor may be used for the purposes of neutralizing frame charging events, for the CCS experiment it is only used operationally to discharge differential charging events. Note that because DSCS-III is an operational satellite, the plasma contactor operation was nominally limited to one firing with a fixed interval of 1 h per 24-h orbit.

D. CCS Control Electronics

The primary purpose of the CCS controller is to determine from onboard processing of SPM data charging levels that trigger activation of the Xe plasma contactor in order to neutralize the differentially charged surface. Additionally, the controller monitors the stability of the contactor operation and deactivates the source after a predetermined time-out, set at 1 h for the CCS experiment. Though the CCS may be configured to be triggered by either a differential charging event (with data coming from one of the SPMs) or by a frame charging event (with data coming from the ion ESA), the CCS experiment made exclusive use of the Kapton-covered SPM as the contactor source trigger. The trigger level was initially set at 1000 V negative (from the baseline voltage), but after June 15, 1998, it was increased to 2500 V to conserve plasma contactor gas.

E. Electrostatic Analyzers

The ESAs used on DSCS-III were originally designed for the low earth orbit environment, but they were modified for application in the GEO environment. The SSJ/4 ESA [17] is a cylindrical plate analyzer that can be configured to detect electrons or ions, and the energy range of the particles to be analyzed varies nominally from 30 eV to 30 keV in 20 logarithmically spaced energy channels. To cover this energy range, two pairs of concentric cylindrical plates are employed: one with a 127° curvature (for the 30-eV to -1.0-keV particles), and one with a 60° curvature (for the 1.0- to 30-keV particles). Because previous studies have shown that electrons with energies as high as 50 keV may be responsible for significant differential surface charging [9], the electron ESA was modified to span the energy range from 20–50 keV. The ESAs include the cylindrical plates, channel electron multipliers (CEMs) for charge multiplication, precision high voltage generators to drive the analyzer plates and provide bias to the detectors, and output logic to interface with the spacecraft. For the CCS experiment, the ion ESA was configured to measure fluxes from 17 eV to 12.3 keV in 31 logarithmically spaced channels, whereas the electron ESA provided fluxes integrated over 20–50 keV.

IV. CCS Observations

An example of spacecraft charging and particle fluxes seen during one complete 24-h orbit appears in Fig. 2. Here, the data appear for day 242 (August 29) of 1996, starting from midnight UT (20:30 MLT). In the top panel of the figure, ion spectra are plotted as a function of time (x scale) and differential in energy (y scale). The color scale on the right of the panel applies to the flux intensity of the ions, given in units of particles per square centimeter per second per electron volt. From the ion spectra, the spacecraft frame-to-plasma potential can be determined using the so-called ion peak method, using the principal that ions from the background plasma will be accelerated through the potential drop that exists between the charged body and the plasma [18]. For example, in the ion spectra data, there is a prominent peak that begins at approximately 18 700 s (05:11) UT with a peak in the ion flux in the 300-eV energy channel, thus corresponding to a –300-V frame potential. This frame charging event slowly decreases in time until it reaches a level of −81 V at 25 260 s (07:01) UT, where it remains negligible until the next event of the day, beginning at 30 485 s (08:28) UT.

The middle panel of Fig. 2 is a relative measure of plasma current escaping the Xe plasma contactor during source activation. The lower panel of the figure displays traces color coded in the legend and are described from left to right as follows: 1) the white trace represents the electron count integrated over the energy range from 20–50 keV; 2) the green trace represents the SPM 1 (Astroquartz) voltage; 3) the red trace represents the SPM 2 (Kapton) voltage; 4) the blue represents the SPM 1 sun sensor (SS1); 5) the cyan trace represents the SPM 2 sun sensor (SS2), and 6) the orange trace represents the on/off state of the Xe plasma contactor. The left y- axis represents the electron count, and the right y axis represents the SPM voltages (in volts). Note that the SPMs have been calibrated to span the voltage range from 1000 V positive to 4000 V negative [8];

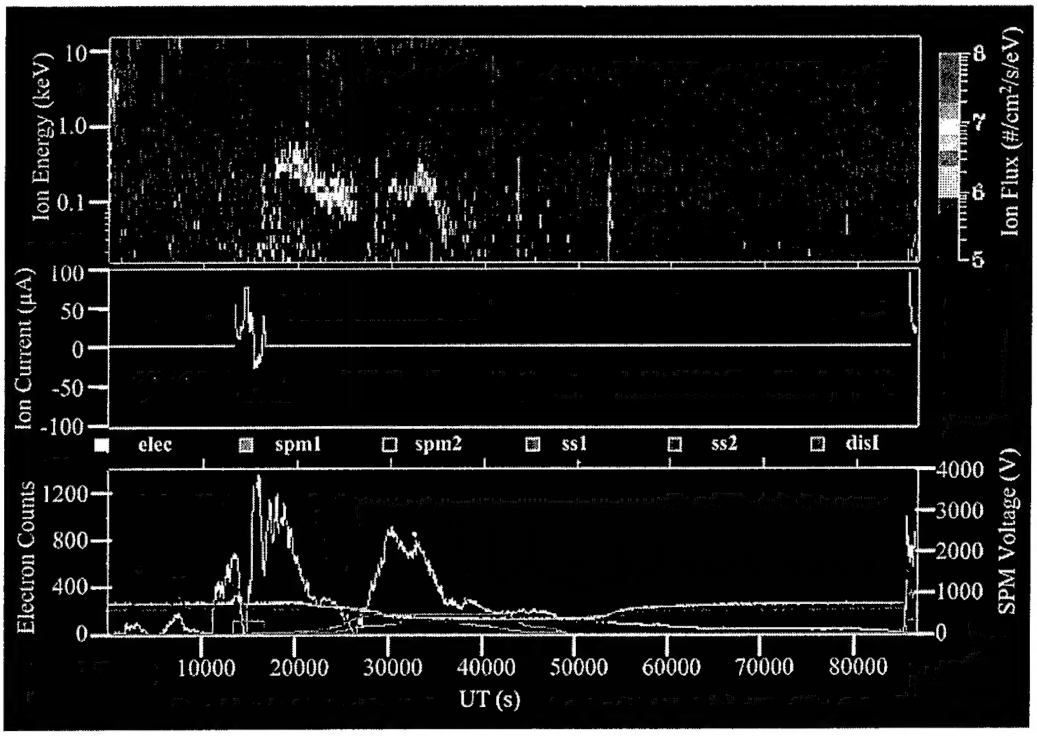

Fig. 2. DSCS-III B-7 surface charging and particle observations appear over a 24-h period, beginning at midnight UT (20:30 MLT). Data for August 29, 1996 are shown here. The top panel indicates ion fluxes differential in energy. The middle panel shows the plasma thruster current, and the bottom panel indicates the SPM voltages, electron counts, sun sensor illumination, and thruster current. A more detailed description appears in the text.

additionally, offsets in the zero value reduced the range of the negative voltage. In this example, there is a significant peak in the charging electrons at 13 475 s (03:44) UT associated with a Kapton (SPM2) voltage of approximately 1640 V, or 1000 V above its uncharged value. During this stage of the mission, the plasma contactor was configured to activate with a trigger based on the charging of Kapton above 1000 V (in magnitude) over its quiescent state. Almost immediately after activation of the contactor, the Kapton potential dropped to less than half of its original value in spite of the continued presence of large fluxes of electrons. As the contactor initiated, the plasma current peaked with net positive charge flow and remained positive until a large influx of electrons from the environment came in at 15 205 s (04:13) UT. With this dramatic increase in negative charges to the spacecraft frame, the net flow of charge from the spacecraft through the thruster became negative and remained so until the external electron source decreased significantly at approximately 16 200 s (04:29) UT.

The distribution of differential charging events was studied for the period covering day 229, 1995 through day 165, 2001. The peak voltages for each SPM and the corresponding electron counts were recorded for each day, along with days in which larges fluxes of electrons were observed in the absence of significant SPM voltages. Because even a small amount of sunlight incident on the SPMs provides enough photodesorption of any bulk static charge, days in which electron fluxes were present during times when the SPMs were exposed to sunlight were not considered in this study. The convention for specifying key quantities, including the SPM baseline voltage, the prethruster firing peak voltage, the "neutralization voltage" resulting from plasma contactor activation and the peak daily voltage is illustrated in Fig. 3.

V. Differential Charging Statistics

A histogram of differential charging data accumulated over the study period (Fig. 4) illustrates the frequency of charging events, defined as periods during which the SPMs charged to greater than 200 V negative over the baseline voltage, and its dependence on local time. The observed local time dependence is similar to that observed during the SCATHA mission [9] and for DSCS-III frame charging [4] and is temporally correlated with the injection of charging electrons in the ambient GEO environment. Note here that a significant majority (>95%) of the events occur within a 5-h time period—a narrower band in time compared to that of DSCS-III frame charging. This is due to the regular exposure of the materials to sunlight between 0700–1500 UT. Events between 1500–2100 UT are rare due to the lack of charging electrons in GEO during those local time [4].

The occurrence of differential charging over the entire study period is shown in Fig. 5. For both Astroquartz and Kapton, the 30-day running average of daily maximum charging level is plotted versus day number. We immediately note the consistently larger Kapton charging levels over those of Astroquartz. Furthermore, a seasonal periodicity is evident in the data, indicative of the favorable geometry of the geomagnetic field for geomagnetic activity leading to the injection of hot electrons into the GEO environment (the so-called Russell-McPherron effect—see [19]). Finally, we note a general trend of increasing charging activity the mission proceeds from solar minimum

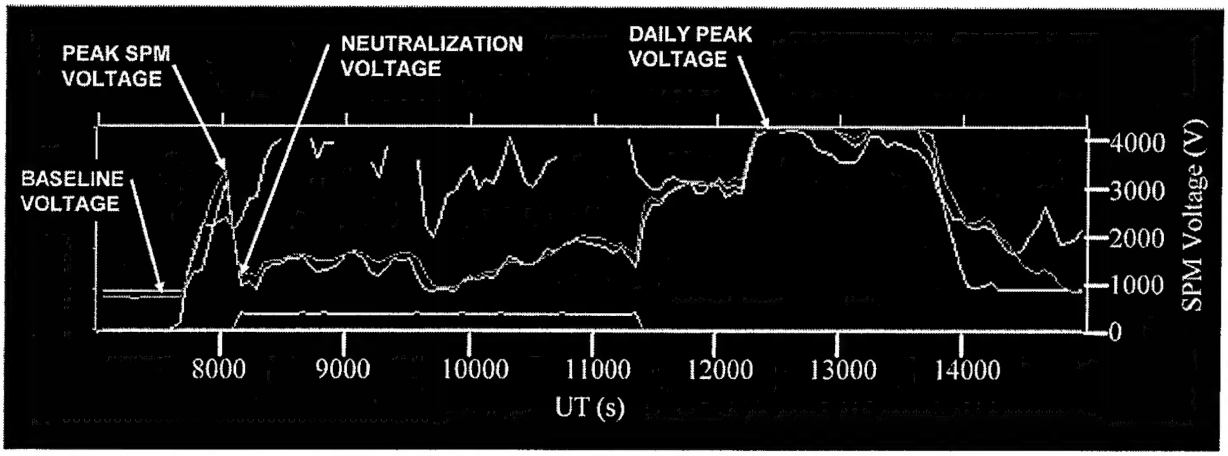

Fig. 3. Differential charging event is characterized by the prethruster-firing peak in the SPM followed by a neutralization voltage. Daily values include the baseline voltage and the peak SPM voltage, saturated in this example. Labeled here are the values for Kapton (red trace) for this particular event (April 25, 1998).

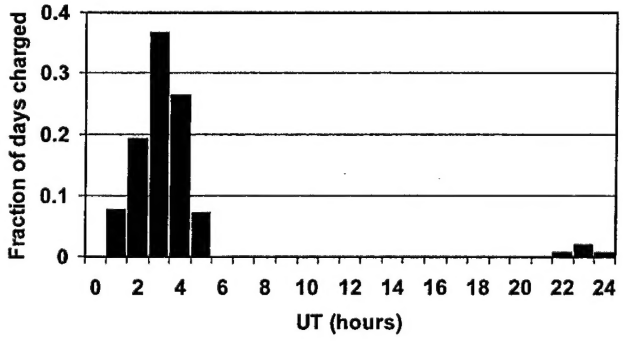

Fig. 4. Histogram illustrating the relative fraction of charging events categorized in time. Recall midnight MLT ⇔ 03:30 UT.

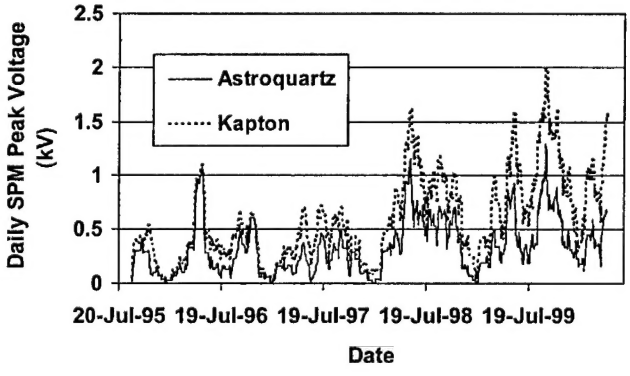

Fig. 5. Thirty-day moving average of SPM voltages for the duration of the study.

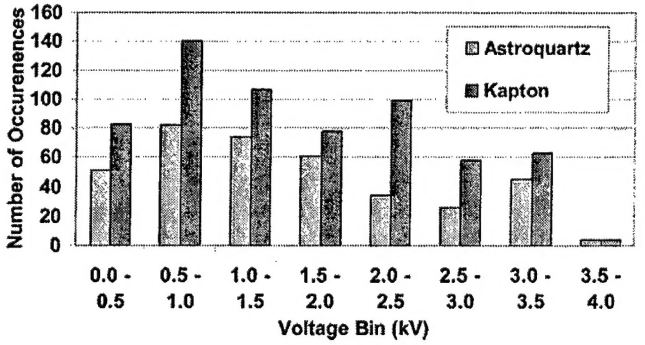

Fig. 6. Histogram of charging events for duration of the study, categorized by voltage level. The susceptibility of Kapton to differential charging is evident by the greater number of events over all charging levels.

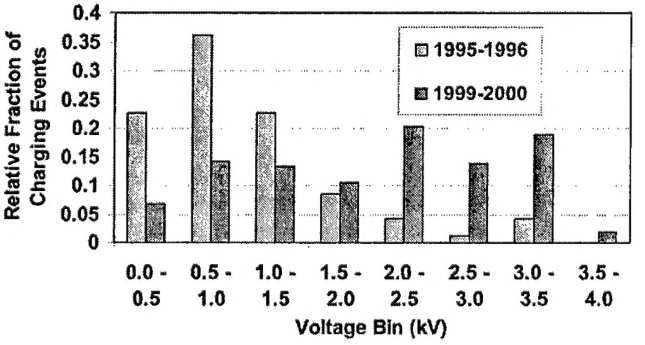

Fig. 7. Histogram of Astroquartz fractional charging levels toward the beginning and end of the study period. Solar cycle effects are seen here, with the greater percentage of charging events being at low levels during solar minimum (1995–1996) and at higher levels during solar maximum (1999–2000).

(1995) toward solar maximum (2000). The apparent correlation between solar/seasonal effects and the periodic features in the data suggests a strong link between geomagnetic activity and differential surface charging, consistent with other studies (e.g., [4]).

The distribution of the charging events is sorted by voltage levels for the duration of the study period and is illustrated in Fig. 6. Here, we see that the number of events is greater for the Kapton sample than for Astroquartz at all voltage levels. When the distribution is further broken down by position in the solar cycle (see Figs. 7 and 8), we see that whereas both Kapton and Astroquartz reach higher levels during the solar maximum periods, the effect is particularly more pronounced for the Kapton sample. Furthermore, the event-specific Astroquartz-to-Kapton voltage ratios for major peaks (> 500 V negative above baseline) in the data were sorted for 1997 (solar declining phase) and 2000 (solar max), as illustrated in Fig. 9. Note that in a solid majority of events (>55%) the Astroquartz was completely uncharged during Kapton charging events. Fewer than 8% of

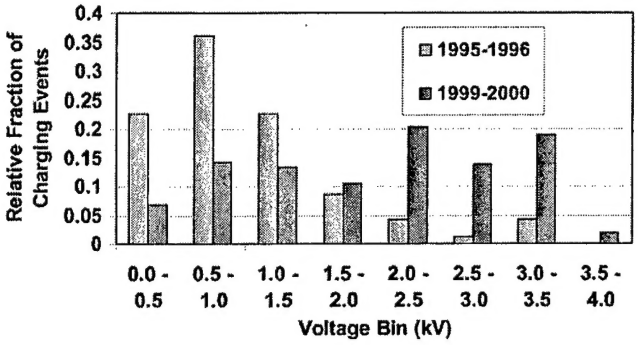

Fig. 8. Histogram of Kapton fractional charging levels toward the beginning and end of the study period. Solar cycle effects are again seen here, but the distinction is more prominent for the Kapton sample than the Astroquartz seen in the previous Figure.

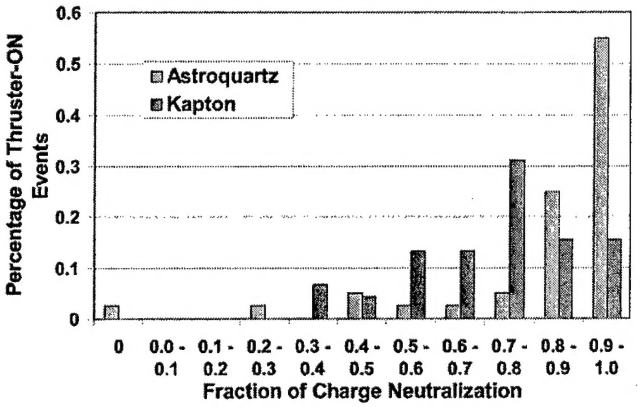

Fig. 10. Histogram illustrating the Xe plasma contactor neutralization efficiency of Astroquartz and Kapton for 1997 (solar declining phase).

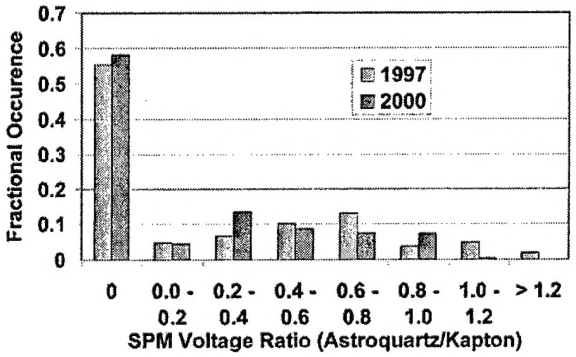

Fig. 9. Histogram showing the ratio of peak daily voltages between Kapton and Astroquartz for 1997 and 2000.

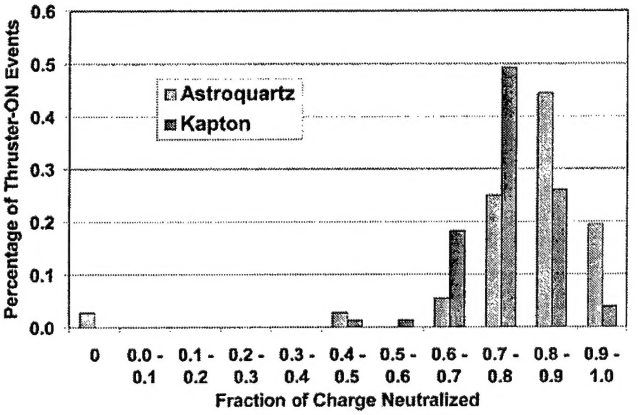

Fig. 11. Histogram illustrating the Xe plasma contactor neutralization efficiency of Astroquartz and Kapton for 2000 (solar maximum).

events resulted in Astroquartz charging to higher levels than Kapton, and of the more than 600 events that were considered here, there were no occurrences of Astroquartz charging in the absence of Kapton charging. Also note that disparity increased in severity during solar maximum conditions, where less than 1% of events with Astroquartz charged to greater levels than Kapton and the statistics in general are skewed toward lower values. Clearly, material effects are significant and must be considered in addition to the environmental effects shown in Fig. 5.

The efficacy of the Xe plasma contactor in the neutralization of the dielectrics is illustrated in Figs. 10 and 11. In Fig. 10, a histogram shows the distribution of the reduction of voltage after contactor firing for both SPM materials for 1997 (solar declining phase). Here, we see that over 55% of the Astroquartz charging events were reduced by over 90% of their original charged value. Kapton was more resilient against neutralization, resulting in only 15% of the events being neutralized by 90% or more. Nonetheless, the contactor still proved useful to even Kapton, with over 60% of events reduced in voltage by over 70% of its original value. During the solar maximum period, illustrated in Fig. 11, we see that even fewer events—less than 5%—were reduced by 90% for the Kapton sample, though almost 80% of the events resulted in a reduction in voltage by 70% or more.

Fig. 12 illustrates a charging event that is clearly modulated by the charging electrons. Such features are readily seen in the data, so there is a clear connection between incident electron flux and SPM voltage levels, often with not much of a discernable time lag. In this particular example, even though there is a significant amount of electrons incident on the spacecraft, because the sensors are coming into sunlight, the SPM voltage modulation by the electrons ceases. Fig. 13 illustrates the relationship between electron fluence to the spacecraft and the SPM voltages averaged for that electron count bin. Again, we see the generally larger sensitivity of the Kapton sample to charging electrons than that of the Astroquartz sample. Furthermore, on average, greater numbers of incident electrons result in higher charging levels. However, with the large variance in the data as represented with the uncertainty bars, the event-specific correlation is so weak that with any given electron count the actual SPM voltage could literally be anything within the range of the sensor. This is further emphasized with the attempt to find a correlation between electron count and Kapton (SPM2) voltage level for events of 1997 (see Fig. 14). Though a more rigorous determination of the contingency table skill score to determine the hit-miss-false alarm rates is necessary for a solid assessment of the utility of an electron sensor, it is apparent from this analysis that electrons will not prove useful as an event-specific proxy of SPM levels.

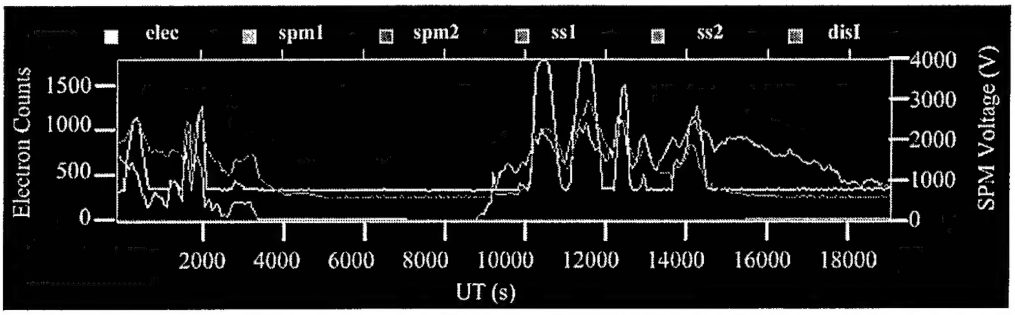

Fig. 12. SPM voltage modulation by incident electrons is evident, especially between 10 000–14 500 s UT.

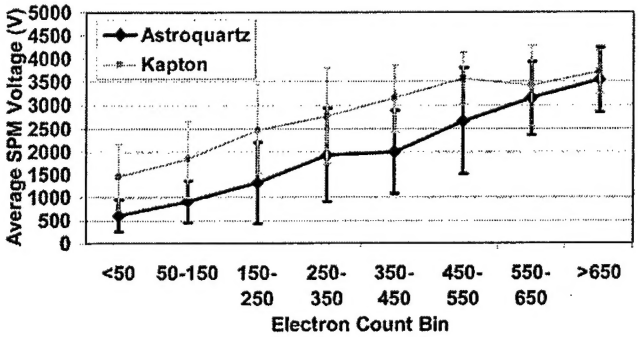

Fig. 13. Average SPM voltages for both Astroquartz and Kapton increase with increasing electron fluence. However, with the large amount of variance in the data, evident from the uncertainty bars representing one standard deviation from the mean, this correlation does not translate into a useful relationship on an event-by-event basis.

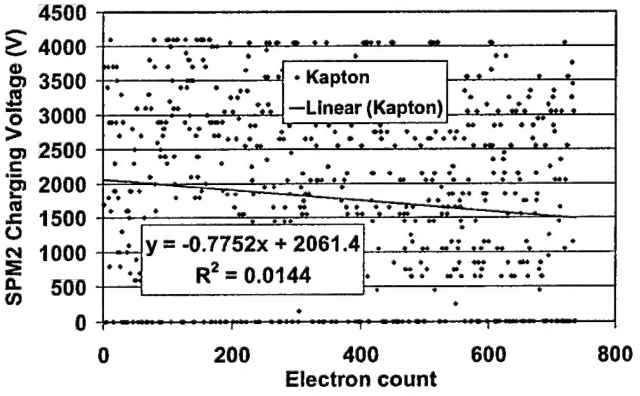

Fig. 14. Correlation between electron counts and Kapton SPM2 Vvoltage levels are plotted for each differential charging event in 1997. Also plotted is the best linear fit to the data, with a correlation coefficient of 0.0144.

VI. Summary of Findings

Six years of differential charging of two materials common to spacecraft, Kapton and Astroquartz, data have been analyzed with surface potential monitors aboard the geosynchronous DSCS-III B-7 spacecraft. Seasonal and solar cycle effects suggest the increase in likelihood and severity of events for both dielectric samples with increased geomagnetic activity. That Kapton becomes increasingly more prone to charging as solar maximum is approached suggests that any dark conductivity increase in the material (if indeed there is any with this specific polymetric composition) is overwhelmed by the severe intensity of charging electrons during this phase of the solar cycle.

Based upon the findings in this study, we have found that, whereas there is a general increase in probability of differential charging with an increase in the so-called charging electron population (i.e., those with energies between 20–50 keV), with the overwhelming variance in the event-specific correlationships observed between these quantities, an electron sensor may not be the ideal sensor for a spacecraft differential charging alarm system. The weak correlation between electron count and differential charging level, the variability in the susceptibility of materials to differential charging, which itself evolves with increased exposure to space radiation, and an observed absence of charging electrons during certain charging events (though rare) cast doubt on the utility of an electron sensor for such a system.

We propose that a single SPM with a judicious choice of dielectric would serve well as a differential charging alarm monitor. Of the two materials used in this experiment, it is clear that Kapton is more likely to charge than Astroquartz at geosynchronous altitudes. Furthermore, because Kapton is more resilient against neutralization by a plasma contactor, it is ideally suited as a "worst case" diagnostic for efficacy of such an active charge control system. If the plasma contactor is successful in neutralizing the Kapton, then neutralization of the Astroquartz is assured. In general, the SPM material for any given spacecraft should be selected in a similar manner based upon comparison with other spacecraft materials. Suggestions for future work include a detailed modeling study with NASCAP-2K of the response of the DSCS-III surface materials to the GEO environment, laboratory studies of the material properties of dielectrics when exposed to space radiation, and a modeling investigation (e.g., with Monte Carlo techniques) of the charge carrier flow within dielectrics that are not so "well-behaved"—such as Astroquartz. These details are critical for the establishment of design criteria that would minimize the impact of differential surface charging on satellite systems.

References

[1] L. Levy, J. M. Siguier, R. Reulet, and D. Sarrail, "Discharges triggered on and by electron bombarded dielectrics," *IEEE Trans. Nucl. Sci.*, vol. 38, pp. 1635–1640, Dec. 1991.

[2] A. R. Fredrickson, "Upsets related to spacecraft charging," *IEEE Trans. Nucl. Sci.*, vol. 43, pp. 426–441, Apr. 1996.

[3] I. Katz, V. A. Davis, M. J. Mandell, D. L. Cooke, R. Hilmer, and L. H. Krause, "Forecasting satellite charging: Combining space weather and spacecraft charging," in *Proc. 38th Aerospace Sciences Meeting and Exhibit*, Reno, NV, Jan., 10–13 2000, AIAA 2000-0369.

[4] L. H. Krause, B. K. Dichter, D. J. Knipp, and K. P. Ray, "The relationship between DSCS-III sunlit surface charging and geomagnetic activity indices," *IEEE Trans. Nucl. Sci.*, vol. 47, pp. 2224–2230, Dec. 2000.

[5] M. J. Mandell, D. L. Cooke, V. A. Davis, G. A. Jongeward, R. A. Hilmer, B. M. Gardner, K. P. Ray, S. T. Lai, M. J. Mandell, and L. H. Krause, "Modeling the charging of geosynchronous spacecraft using NASCAP2K," Adv. Space Res., 2004, to be published.

[6] H. A. Cohen *et al.*, "P78-2 satellite and payload responses to electron beam operations on March 20, 1979, spacecraft charging technology," Air Force Res. Lab., Wright Patterson Air Force Base, OH, AFRL-TR-81-0270, N. J. Stevens and C. P. Pike, Eds., 1981.

[7] E. G. Mullen, A. R. Frederickson, G. P. Murphy, K. P. Ray, E. G. Holeman, D. E. Delorey, R. Robson, and M. Farar, "An autonomous charge control system at geosynchronous altitude: Flight results for spacecraft design consideration," *IEEE Trans. Nucl. Sci.*, vol. 44, pp. 2174–2187, Dec. 1997.

[8] B. K. Dichter, K. P. Ray, M. S. Gussenhoven, E. G. Holeman, D. E. Delorey, and E. G. Mullen, "High voltage frame and differential charging observed on a geosynchronous spacecraft," in *Proc. 6th Spacecraft Charging and Technology Conf.*, Sept. 1, 2000, AFRL-VS-TR-20 001 578.

[9] E. G. Mullen, M. S. Gussenhoven, D. A. Hardy, T. A. Aggson, B. G. Ledley, and E. Whipple, "SCATHA survey of high-level spacecraft charging in sunlight," *J. Geophys. Res.*, vol. 91, pp. 1474–1474, 1986.

[10] A. R. Fredrickson, D. B. Cotts, J. A. Wall, and F. L. Bouquet, "Spacecraft dielectric material properties and spacecraft charging," in *Progr. Astronaut. Aeronaut.*, vol. 107, 1986.

[11] M. S. Leung, M. B. Tueling, and P. F. Mizera, "Long-term light-induced changes in dark conductivity of Kapton,", Air Force Syst. Comm. Rep. SD-TR-84-41, ADA148791, 1984.

[12] H. C. Koons, J. F. Fennell, and D. F. Hall, "A summary of the engineering results from the aerospace corporation experiments on the SCATHA spacecraft," in *Proc. 6th SCTC*, Sept. 1, 2000, AFRL-VS-TR-20001578.

[13] M. S. Leung and H. K. A. Kan, "Laboratory study of the charging of spacecraft materials," *J. Space Rockets*, vol. 18, no. 6, pp. 510–514, 1981.

[14] R. R. Robson and W. S. Williamson, "Flight model discharge Ssystem scientific report no. 4," Air Force Geophys. Lab., Hanscomb AFB, MA, AFGL-TR-88-0150, 1988.

[15] L. H. Krause, "The interaction of relativistic electron beams with the near-earth space environment," Ph.D. thesis, Univ. Michigan, Ann Arbor, 1998.

[16] J. C. Sturman, "Development and design of three monitoringinstruments fo spacecraft charging," NASA, Greenbelt, MD, Tech. Paper 1800, 1981.

[17] T. L. Schumaker, D. A. Hardy, S. Moran, A. Huber, J. McGarity, and J. Pantazis, "Precipitating ion and electron detectors (SSJ/4) for the block 5D/flight 8 DMSP satellite," Air Force Geophys. Lab., Hanscomb AFB, MA, AFGL-TR-88-0030, 1988.

[18] P. F. Mizera, "Charging results from the satellite surface potential monitor," *J. Spacecr. Rockets*, vol. 18, no. 6, pp. 506–509, 1981.

[19] M. G. Kivelson and C. T. Russell, *Introduction to Space Physics*, ser. Cambridge Atmospheric and Space Science Series. Cambridge, U.K.: Cambridge Univ. Press, 1995.